Fortgeschrittenen-Praktikum I
Albert-Ludwigs-Universität Freiburg

Report of the Experiment with

Semiconductors

Jan Hofmann Frank Sauerburger

25. und 26. September 2013

jan@meinanolis.de
frank@sauerburger.net

Tutor: Christopher Betancourt
christopher.betancourt@physik.uni-freiburg.de
phone: 5933

Contents

Introduction **3**
0.1 Motivation . . . 3
0.2 Theoretical Basics . . . 3
0.2.1 Semiconductor . . . 3
0.2.2 Band Model . . . 3

1 Band Gap **5**
1.1 Introduction . . . 5
1.1.1 The Set-Up . . . 5
1.1.2 Theoretical Basics . . . 5
1.2 Measurement . . . 7
1.2.1 Germanium . . . 7
1.2.2 Silicon . . . 8
1.3 Evaluation . . . 9
1.4 Conclusion . . . 11

2 Haynes & Shockley Experiment **13**
2.1 Introduction . . . 13
2.2 Measurement . . . 14
2.2.1 Variation of Position x . . . 14
2.2.2 Variation of External Electrical Field E . . . 15
2.2.3 Estimation of Errors . . . 15
2.2.4 Variation of External Electrical Field E . . . 15
2.3 Evaluation . . . 15
2.3.1 Variation of Position x . . . 16
2.3.2 Variation of External Electrical Field E . . . 21
2.4 Discussion of the Results . . . 25
2.5 Conclusion . . . 25

3 Semiconductor Detector **27**
3.1 Introduction . . . 27
3.1.1 Set-Up . . . 27
3.1.2 Theoretical Basics . . . 27
3.2 Measurement . . . 28

3.3 Evaluation 28
3.3.1 Calibration of Channels 29
3.3.2 Proportion of Absorption 31
3.3.3 Relative Energy Resolution 31
3.4 Conclusion 32
3.4.1 Calibration Line 32
3.4.2 Proportion 32
3.4.3 Relative Energy Resolution 33

A Part I **35**

C Part III - Si **39**

Introduction

0.1 Motivation

This experiments goal is to lead the student into the world of semiconductors. A field in todays technology of immense importance. Therefore three experiments will be done. The first experiment gives a deeper view on the band gaps. Those we will measure. The second experiment, the Haynes and Shockley-Experiment, gives us an introduction on the behaviour of electrons in a n-dotted semiconductor. Here we gain a grasp for quantities as lifetime, diffusion and moveability. The third experiment is about semiconductor detectors. Here we examine the characteristics of different semiconductors with γ-rays.

0.2 Theoretical Basics

0.2.1 Semiconductor

A Semiconductor is a solid which depending on its state has conducting or isolating attributes. Depending on the temperature the specific resistance ρ is between 10^8 to $10^{-3}\Omega/\text{cm}$.

$$\rho = R \cdot \frac{A}{l} \tag{1}$$

Here R names the resistance, A the intersection and l the length of the semiconductor. For higher temperatures there are more quasi free electrons (=electrons in the conducting band) which can participate in the current, which reduces the resistance.

0.2.2 Band Model

To describe the conductivity of a crystal it is useful to use the band model. Electrons have discrete energy levels within the coulomb potential of a signal atoms which is proportional to $1/r^2$. If the atoms are close enough together as it is in many crystals these potentials overlap and the energy levels of the electrons merge to quasi continuous levels, called so called bands. This is often referred to as the Bloch's theorem. At 0 Kelvin all level in the bands below the Fermi-energy are

occupied by electrons. The last filled band is called valence band. The one above is the conducting band. A γ-ray delivers energy to an electron via photo- or Compton-effect, so that it can be lifted into the conducting band. If a field is applied on the crystal this electron will be accelerated. At the point where the electron was lifted, a so called hole emerges, which is treated as a particle which positive charge.

Part 1

Band Gap

1.1 Introduction

1.1.1 The Set-Up

In figure 1.1 one can see the set-up of the first experiment. With this set up we are able to measure the spectrum of absorbed and transmitted light in the semi conductor. We have a lamp which emits light with a continuous spectrum. Whether the intensity of the lamp is constant for each color we will measure later on. Behind the lamp we find a fan called chopper. It cuts the constant beam into pulses of 70Hz. The following lens makes the light monotropic. Now the beam meets a grate which is attached to an rotatable desk. The grate will brake the light depending on its energy. By rotating the desk with the grate attached and adjusting the shutter one can select which color and range of the light reaches further parts of the experiment. Another lens focuses the light onto the pyrodetector. But before arriving there the light passes a filter which selects a rough range of color. This is to prevent higher orders of interferences from the grate to reach the detector. The semiconductor will absorb the light depending on its characteristic and the lights wavelength. The construction of the desk will report its angle to a computer. The pyrodetector and the semiconductor forwards the value of transmission and absorption to an Lock-In Amplifier. It can use the chopped light pulses to split the mixed light of lamp and environment and extract the data without effects of environmental light. The computer captures all this data twice a second.

In this experiment we use two different types of semiconductor Silicon and Germanium with their corresponding grates.

1.1.2 Theoretical Basics

Subtracting the Underground and Normalization

Although we used the Lock-In Amplifier we still have an underground which we need to subtract. Also we need to account that the lamps intensity depends on the

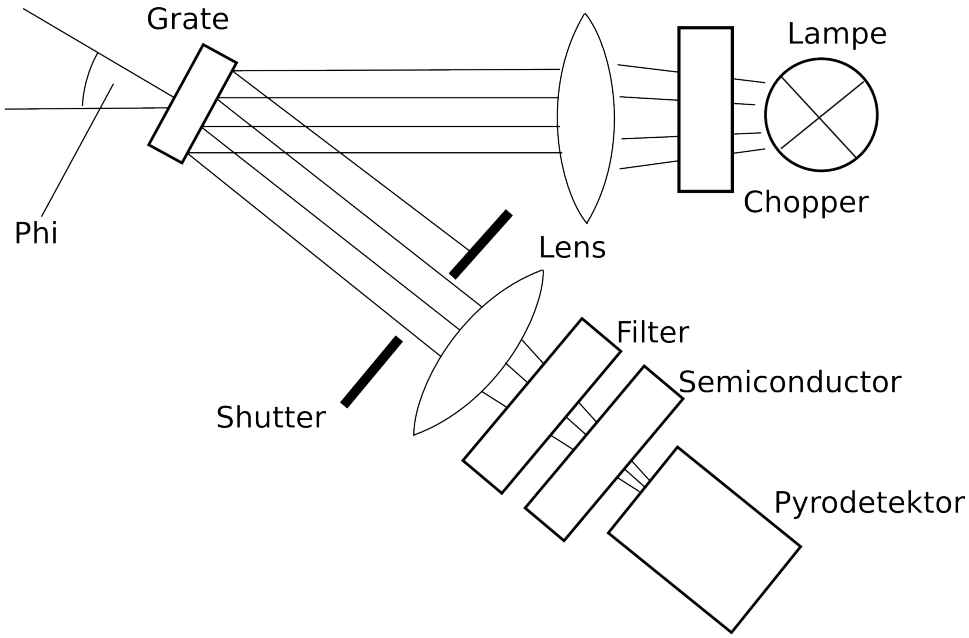

Figure 1.1: Schematic set-up of the first experiment.

wavelength. It is given [3]

$$T = \frac{T_m - U_T}{L} \qquad A = \frac{A_m - U_A}{L} \tag{1.1}$$

with T the real and T_m the measured Transmission, A the real and A_m the measured absorption which all depend on the wave length of the light. U_T and U_A stands for the underground of transmission and absorption. $1/L$ normalizes the signal to the lambs intensity.

Converting Angles and Energies

In the experiment we are measuring the angle. But what we are really interested in is the energy of the photons hitting the semiconductor behind the grate. Therefore we need to convert this. With the lattice parameter, the angle and some natural constants we can transform angle to energy through the law of fraction at a grate[3].

$$E(\phi) = \frac{hc}{2d \cdot \sin(\phi) \cdot \cos(\psi)} \tag{1.2}$$

ϕ	measured angle by rotating desk
ψ	half angle between beam before and after grate $\psi = 7.5°$
h	Planck-constant
c	speed of light
d	lattice parameter

For our grates we have the lattice parameter of $d_{Ge} = \frac{1}{600}$mm and $d_{Si} = \frac{1}{1200}$mm [3]. Both are chosen so that the energy of the band gap is approximately at 40°.

1.2 Measurement

1.2.1 Germanium

Settings for the measurements

I	= 15,06 mA
Pyro pre amplification	= 300
Semiconductor pre amplification	= 300

Measurement 1: (Main measurement)

Measuring all angles with complete set-up.[1]

File: `data/band_ Ge.txt`

Measurement 2: (Lamp)

Measuring all angles without semiconductor in the light beam.

File: `data/lampe_ Ge.txt`

Measurement 3: (Underground)

One minute of measurement with covered semiconductor and pyrodetector.

File: `data/unterg_ Ge.txt`
Duration: 60s

[1] All the data files can be found online https://github.com/esel7353/FP-I/tree/master/Halbleiter/data

Measurement 4: (Error)

A single angle for one minute to get an estimation of the error of each measure point.

File: `data/fehler_ Ge.txt`
Duration: 60s

1.2.2 Silicon

Settings for the measurements

I	= 0,74 mA
Pyro pre amplification	= 100
Semiconductor pre amplification	= 30

Measurement 5: (Main measurement)

Measuring all angles with complete set-up.

File: `data/band_ Si.txt`

Measurement 6: (Lamp)

Measuring all angles without semiconductor inside the light beam.

File: `data/lampe_ Si.txt`

Measurement 7: (Underground)

One minute of measurement with covered semiconductor and pyrodetector.

File: `data/unterg_ Si.txt`
Duration: 60s

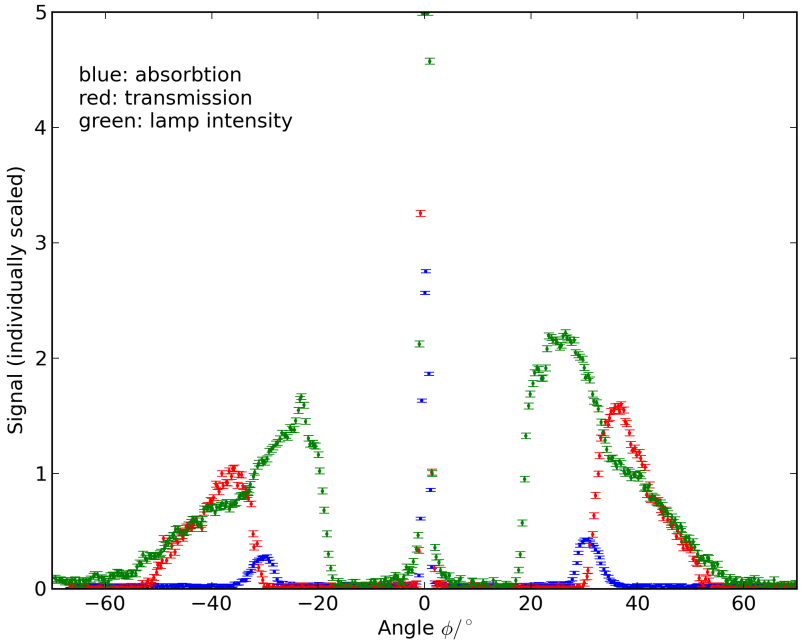

Figure 1.2: Plot of all data as we received it from the computer

Measurement 8: (Error)

A single Angle for one minute to get an estimation of the error of each measure point.

File:	`data/fehler_ Si.txt`
Duration:	60s

1.3 Evaluation

In Figure 1.2 you can see the raw data.[2] One can see that the absorption and transmission spectrum has to be normalized to the lamp intensities – see 1.1. In Figure 1.3 a detailed extract of the left intersection of the real absorption and transmission spectra. As shown in the figure we used the maximum of the transmission and its slope to create two lines which intersect at the very point where the absorption begins. Same we did with the minimum and the slope of the absorption and for the right side of the Germanium measurement. From this we get 4 data points that we can average to get the energy of the band gap. We repeat this for both sides of the Silicon measurements. The plots are shown in the attachment. In the table 1.1 all four data points of Germanium are shown together with their average as well as the same results for the silicon detector.

[2] All fits and plots in this part are done with Python

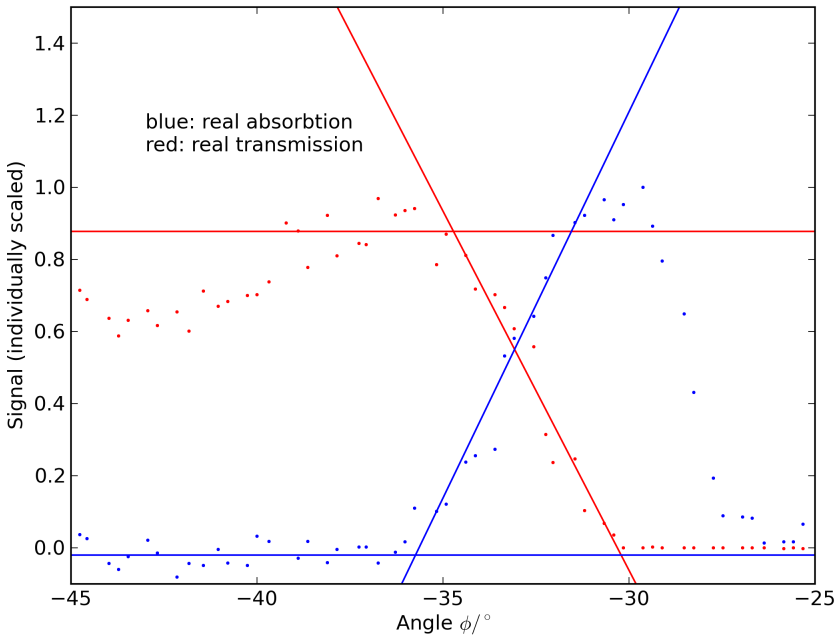

Figure 1.3: All normalized and zoomed to the left crossing of absorption and transmission

	Ge-Detector	Si-Detector
Left Absorption	(35 ± 3)	(42 ± 4)
Left Transmission	(36 ± 3)	$(45 \pm 1,8)$
Right Absorption	(35 ± 3)	(43 ± 2)
Right Transmission	(36 ± 3)	$(42 \pm 1,9)$
Average	(35 ± 2)	$(44 \pm 1,2)$

Table 1.1: List of intersections for absorption and transmission in Si- and Ge-Detector

We get the error of the measured spectra from a special measurement for only one angle close to the expected band gap energy. The scattering

$$s = \sqrt{\frac{1}{n-1} \cdot \sum_{i}^{n} (x_i - \bar{x})} \tag{1.3}$$

of this measurement will be treated as the uncertainties of the absorption, transmission and lamp spectra. We made the same calculation of scattering to estimate the standard deviation s_U of the underground. When we use Gaussian error propagation on (1.1) we get the standard deviation of the real spectra. Here shown for the absorption.

$$s_A = A\sqrt{\frac{s^2 + s_U^2}{(T_m - U_T)^2} + \frac{s_L^2}{L^2}} \tag{1.4}$$

The error of the transmission is calculated similar.

From the fits of the horizontal line h we get the uncertainty of its value s_h and from the fit of the line $m\phi + b$ we get the errors s_m and s_b. The error s_ϕ of the intersection $\phi_I = \frac{h-b}{m}$ can be calculated with Gaussian error propagation.

$$s_\phi = \sqrt{\left(\frac{s_h}{m}\right)^2 + \left(\frac{s_b}{m}\right)^2 + \left(\frac{h-b}{m^2} s_m\right)^2} \tag{1.5}$$

With equation (1.2) we get the energy of both band gaps and the Gaussian error would be

$$\sigma_E = \frac{hc}{2d \cdot \cos(\psi)} \cdot \frac{2\cos(\phi}{\cos(2\phi) - 1} \cdot \frac{\pi}{180^\circ} \cdot \sigma_\phi. \tag{1.6}$$

The final results are

$$E_{Si} = (1.73 \pm 0.06) \cdot 10^{-19}\text{J} = (1.08 \pm 0.04)\text{eV} \tag{1.7}$$

$$E_{CdTe} = (1.05 \pm 0.05) \cdot 10^{-19}\text{J} = (0.65 \pm 0.03)\text{eV}. \tag{1.8}$$

1.4 Conclusion

Our results for the band gap energy are

$$E_{Si} = (1.08 \pm 0.04)\text{eV}, \tag{1.9}$$

$$E_{Ge} = (0.65 \pm 0.03)\text{eV}. \tag{1.10}$$

The literature values [3] are

$$E_{Si} = 1.12\text{eV}, \tag{1.11}$$

$$E_{Ge} = 0.66\text{eV} \tag{1.12}$$

so for both values we are in agreement within our errors.

Part 2

Haynes & Shockley Experiment

2.1 Introduction

This part of the experiment shows the movement of an electron cloud in an electrical field in a semi conductor. We use the n-doted semiconductor Germanium. From the data we should be able to calculate semi conductor dependent constants such as the moveability μ_n, diffusion constant D_n and life time τ_e of electrons in the semi conductor.

J. R. Haynes and W. Shockley first showed in their experiment that the movement of an electron cloud in a semiconductor can be made visible with an oscilloscope.[3]

To create the electron cloud we use a laser. The laser hits a semi conductor and due to the photo electrical and the coulomb effect it lifts electrons from the valence band into the conducting band. We also apply an electrical field to the semi conductor so the electrons start so move in the field. A few millimeters away from the laser hit point we place a needle which is amplified in the aperture and shifted, what means that a constant voltage is subtracted to produce a signal that we can measure with an oscilloscope in an appropriate measurement range. See figure 2.1

The movement of electrons in an electrical field in a semi conductor can be modeled by the equation[3]

$$c(x,t,E) = Ce^{-\frac{t}{\tau_n}} \cdot \frac{1}{\sqrt{4\pi D_n T}} \exp\left(-\frac{(x-\mu_n Et)^2}{4D_n t}\right) \tag{2.1}$$

where C characterizes the total charge lifted to the conducting band when the laser hits the semi conductor. τ_n is the life time of these electrons in the conducting band, D_n is the diffusion constant, μ_n is the moveability of the electrons and E the electrical field which is present in the semi conductor. The equation models the movement of the center of mass of the electron cloud with a constant velocity $v = \mu_n E$. It also models an exponential decay of the electrons in the conducting

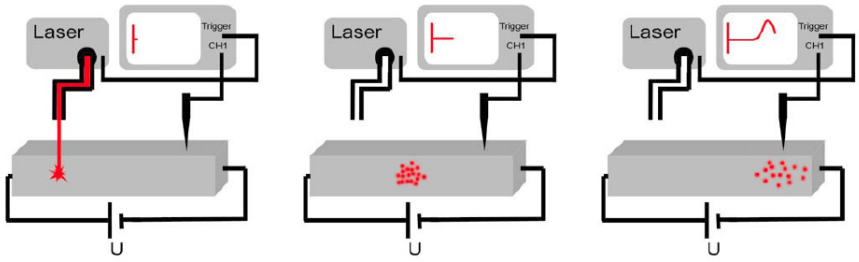

Figure 2.1: Set up of the Haynes and Shockley experiment. The three pictures show the time evolution. First the laser hits the semiconductor and lifts electrons to the conducting band. These electrons start to move due to the external voltage. Finally the electron cloud can be measured with an oscilloscope.

band, which is due to recombination with holes. And the equation also models the diffusion of the electron cloud, which means the cloud gets wider due to the repulsion force of the coulomb field of each electron.

2.2 Measurement

We have made three different measurements, where one had to be repeated. In all measurements we wanted to measure the distance x between the laser hit point and the needle. We have measured the distance x_m between the plastic holder of the fiber optic cable and the plastic holder of the needle. When the two plastic pieces touch each other, there is still a small space between the cable and the needle of $x_0 = (1.27 \pm 0.10)$mm. So the distance x can be calculated with $x = x_m + x_0$. To variate x we can move the fiber optics cable of the laser. In all measurements we have recorded the voltage of the needle $U(t)$ with an oscilloscope. The oscilloscope is triggered by a signal from the laser, so that the oscilloscope starts to recored when the laser hits the semi conductor[1]. We have used a strip of Germanium with a length of $l = (30.00 \pm 0.05)$mm.

2.2.1 Variation of Position x

In this part we have measured the movement of the electrons for a fixed external electrical field $E = U_{\text{ext}}/l$ where $U_{\text{ext}} = (50.4 \pm 2)$V is the voltage which we have applied to the semi conductor and l the total length of the semi conductor. We had to repeat this because in the first measurement the trigger of the oscilloscope was not set correctly – the time $t = 0$ was not that point in time when the laser fired. We will only list the data of out second measurement. Table 2.1 shows the different positions x_m and the corresponding file names[2] of the recorded curves $U(t)$. We

[1] Actually the digital oscilloscope which we have used started to save the voltages a few micro seconds before the laser fires, but the point in time when the laser hits is marked by $t = 0\mu$s.

[2] All files are accessible online https://github.com/esel7353/FP-I/tree/master/Halbleiter/data

x_m/mm	File Name
0.00	`TEK0024.csv`
0.61	`TEK0025.csv`
1.08	`TEK0026.csv`
1.53	`TEK0027.csv`
2.10	`TEK0028.csv`
2.54	`TEK0029.csv`
3.07	`TEK0030.csv`
3.59	`TEK0031.csv`
3.97	`TEK0032.csv`
4.57	`TEK0033.csv`
5.05	`TEK0034.csv`
5.47	`TEK0035.csv`

Table 2.1: Distances and corresponding file names, for which we have recored a $U(t)$ curve. The files are located in the `movX` folder.

could not measure larger distances because of the geometrical limitations of the aperture. The uncertainty of x_m is $s_{x_m} = 0.10$mm.

2.2.2 Variation of External Electrical Field E

In this part the distance between needle and laser $x = (3.2 \pm 0.1)\text{mm} + x_0$ was fixed. Instead we have variated the applied Voltage, so that the external electrical Field $E = U_{\text{ext}}/l$ changes. The uncertainty of the U_{ext} is $s_U = 2\text{V}$. Table 2.2 shows the relation between voltage of external electrical field E and the file name of the data records.

2.2.3 Estimation of Errors

This measurement was intended to be used for the estimation of the errors for this part. Therefore we have measured $U(t)$ curves for a fixed external electrical field $E = U_{\text{ext}}/l = (50.0 \pm 2)\text{V}/(30.00 \pm 0.05)\text{mm}$ and fixed distance $x = (2.65 \pm 0.10)\text{mm} + x_0$. The recorded curves are saved in the files `TEK0036.csv` to `TEK0041.csv` in the folder `mov`.

2.2.4 Variation of External Electrical Field E

2.3 Evaluation

We have made three different measurements. At first we will analyse the measurement where E was fixed and x was variated. And finally we analyse the measurement were E was variated while x was fixed.

U_{ext}/V	File Name
52.8	`TEK0014.csv`
48.0	`TEK0015.csv`
44.0	`TEK0016.csv`
40.0	`TEK0017.csv`
36.8	`TEK0018.csv`
31.2	`TEK0019.csv`
27.2	`TEK0020.csv`
24.0	`TEK0021.csv`
20.8	`TEK0022.csv`
20.8	`TEK0023.csv`

Table 2.2: Applied Voltage and corresponding file names, for which we have recored a $U(t)$ curve. The files are located in the `movE` folder.

We have measured curves for fixed x and fixed E in order to estimate the uncertainties, but due miss conception of this experiment explained in the next section, we can not use this data to estimate the uncertainties.

2.3.1 Variation of Position x

We have measured the voltage $U(t)$ which is proportional to the charge under the needle, for a fixed electrical field $E \propto U_{\text{ext}}$. For every distance x we have measured a function of time t, so according to (2.1) the measured voltage should be proportional to

$$U(t) \propto \frac{C}{U_c} U_{x,E}(t) = c_{x,E}(t) = Ce^{-\frac{t}{\tau_n}} \cdot \frac{1}{\sqrt{4\pi D_n t}} \exp\left(-\frac{(x-\mu_n E t)^2}{4D_n t}\right) \tag{2.2}$$

where the subscript x, E indicates that these parameters are fixed. At this point the problem of the experiment arises. The manual[3] advises us to fit our 'recorded curves' with a Gaussian $c(x) = \frac{1}{\sqrt{2\pi}\sigma} \exp\left(-\frac{1}{2}(x-x_c)^2/\sigma^2\right)$. Unfortunately this is not possible, because the curves we have measured are functions of time t and not of the position x. On can suggest to change the variables and fit a Gaussian $c(t)$, but this isn't a good idea, because our measure cures are not supposed to be Gaussian – (2.2) is clearly not a Gaussian function in t.

We came up with the following solution. We have to make a transformation[3] of our data. For every fixed point in time t we express our data as a function of the manually measured distance x: $U_{t,E}(x)$. Our data set has about 2500 points in time for 12 different values for x. After the transformation we will have 2500 functions $U_{t,E}(x)$ each with 12 data points. According to (2.2) $U_{t,E}(x)$ as function of x is a Gaussian. This means we make a Gaussian fit (2.3) for every point in time

[3]We used Python to transform, fit and plot all the data in this part.

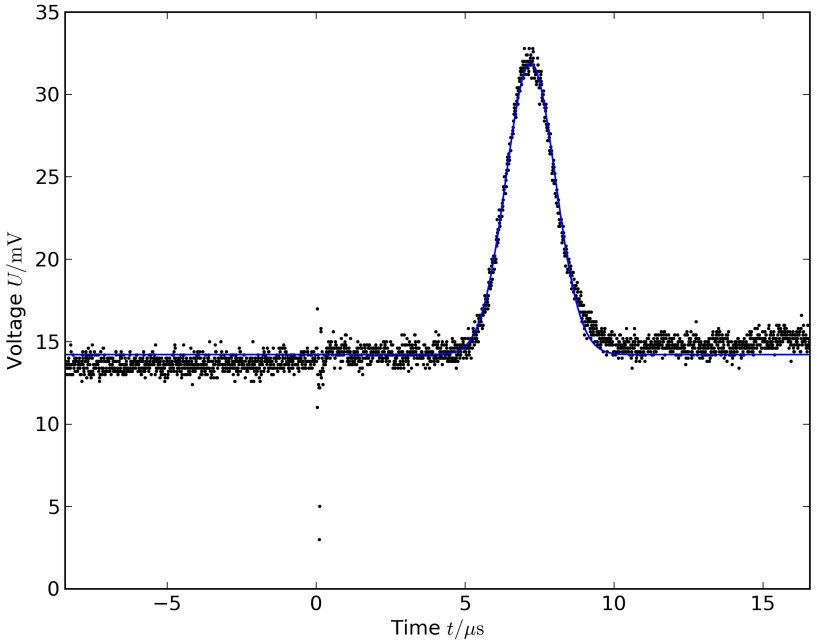

Figure 2.2: Example of our measured curves $U(t)$ for $x = (2.54 + 1.27)$mm with a Gaussian fit. The data points shows the width in time of the electron cloud which is overlapped by the dispersion and the decay.

with the transformed data.

$$U_{t,E}(x) = A \cdot \frac{1}{\sqrt{2\pi\sigma^2}} \exp\left(-\frac{1}{2}\frac{(x-x_c)^2}{\sigma^2}\right) \tag{2.3}$$

Comparing equation (2.3) and (2.1) we get the following relations

$$\begin{aligned} x_c &= x_c(t) = \mu_n E t \\ \sigma &= \sigma(t) = \sqrt{2D_n t} \\ A &= A(t) = Ce^{-\frac{t}{\tau_n}} \end{aligned} \tag{2.4}$$

which of course are functions of t. The relations (2.4) are in agreement with the manual[3].

In reality the transformation was not that easy as one could assume form above. Our measured curves were shifted individually (shifted output). This means we have to fit a Gaussian plus offset (2.5) to out measured curves, even if the Gaussian is not true.

$$U_{x,E}(t) = C \cdot \frac{1}{\sqrt{2\pi\sigma^2}} \exp\left(-\frac{1}{2}\frac{(x-x_c)^2}{\sigma^2}\right) + o \tag{2.5}$$

An example of these fits is shown in figure 2.2.

We then subtracted the offsets o from all the curves $U(t)$ and transform them

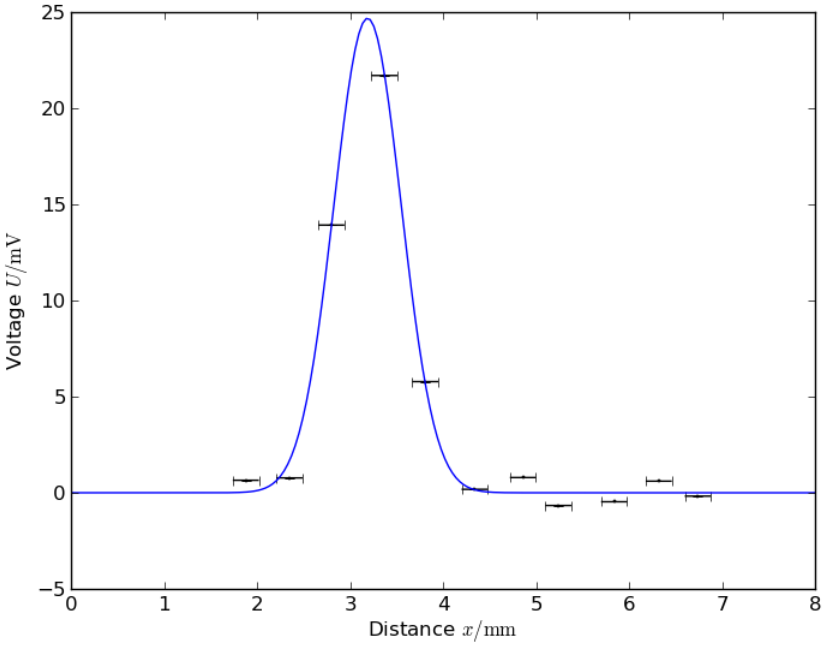

Figure 2.3: Example of the transformed function $U(x)$ for $t = 6.02\mu$s. This shows the spacial width of the electron cloud.

as explained above. Due to different measuring ranges for different positions x, not every curve had a value for a certain point in time. We decided to use only those points in time where the oscilloscope has measured a value for at least 11 different values of x. This means the transformed functions $U(x)$ have at leased 11 data points. The error can be calculated with Gaussian error propagation of the position is $s_x = \sqrt{2 \cdots \frac{2}{x}} = 0.14$mm. We fitted a Gaussian (2.3) to these functions. An example is shown in figure 2.3. Each of these fits produce the values $A(t)$, $\sigma(t)$ and $x_c(t)$ (and standard deviations for each) for a certain point in time t. These values are shown in the figures 2.4, 2.5 and 2.6 .

The curves $U_{Et}(x)$ have 11 or 12 data points which have quite large uncertainties of x. The voltages are also modulated by a noise. This means the fits might not be that accurate and we expect large scattering. Especially for small times when the electron cloud has not even reach the nearest needle position, the computer tries to fit a Gaussian to the random noise, which leads to random values in a very wide range. The same applies for large times, when the signal is so small that it can not be distinguished from the noise. We can not check that large amount of fit results manually, so we decided to use filter rules to reject some fit results. Each fit results has to pass $t \in [2\mu\text{s}, 1\text{s}] \wedge x_c \in [0.1\text{mm}, 8\text{mm}] \wedge \sigma \in [0\text{mm}, 3\text{mm}] \wedge A \in [0\text{Vmm}, 0.10\text{Vmm}]$. Looking at the figures 2.4, 2.5 and 2.6 one sees that these rules have not been too strict, that only the random fits of the noise have been rejected.

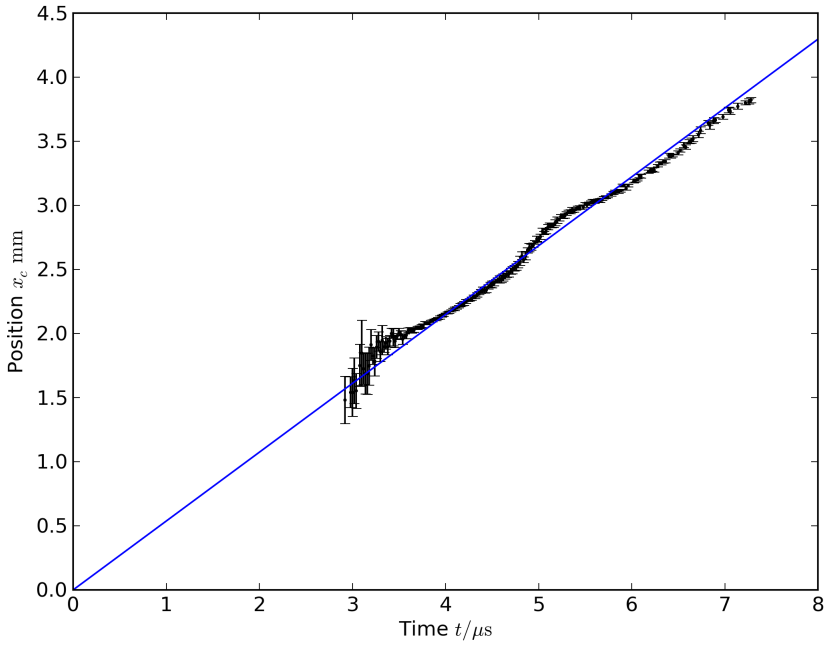

Figure 2.4: Movement of the center of mass of the electron cloud. Fitted with a line trough the origin.

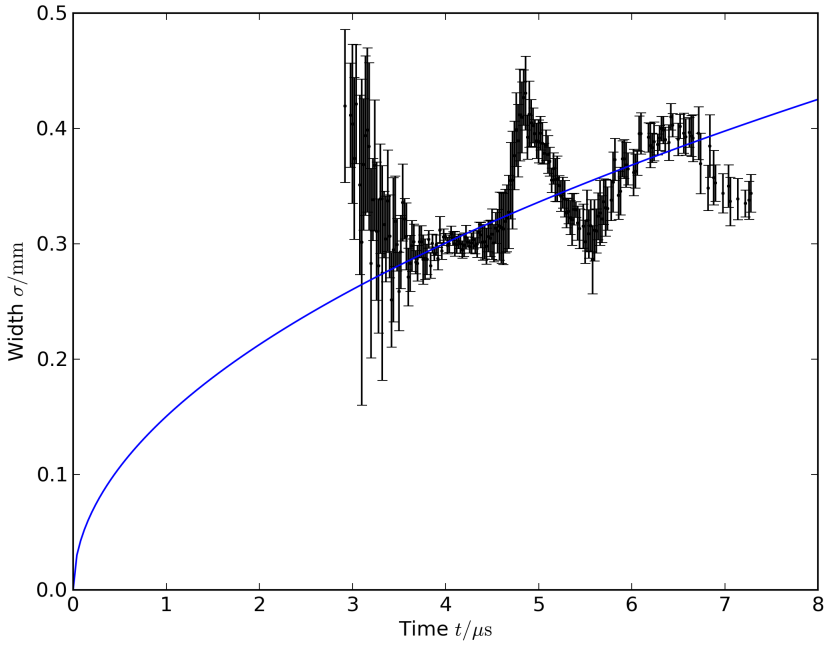

Figure 2.5: Widening of the electron cloud, fitted with a square root.

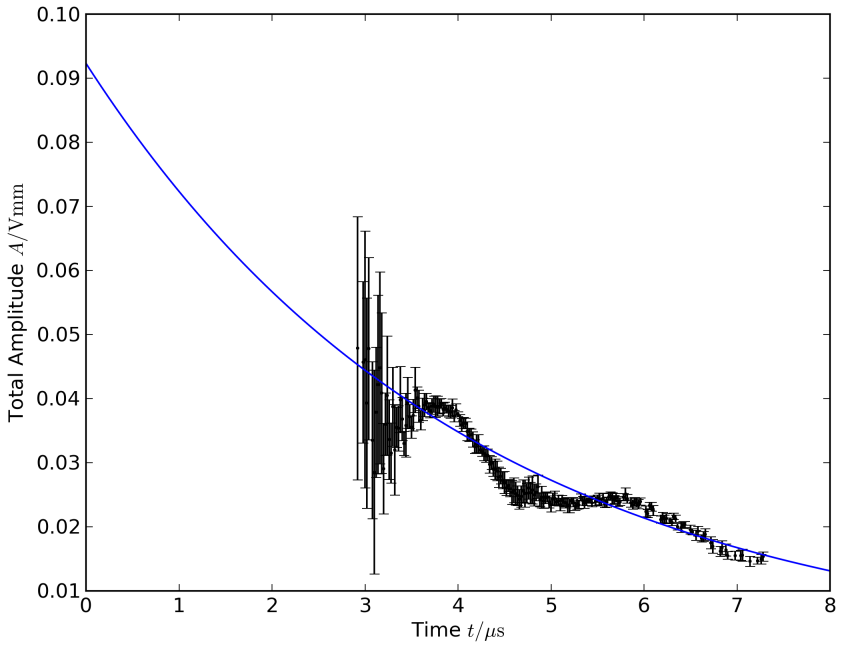

Figure 2.6: Time evolution of the total number of electrons moving, fitted with an exponential decay.

We have fitted these three data sets with the following functions.

$$\begin{aligned} x_c(t) &= vt \\ \sigma(t) &= \sqrt{2D_n t} \\ A(t) &= A_0 e^{-\frac{t}{\tau}} \end{aligned} \tag{2.6}$$

The interested parameters of these fits and their errors are as listed in (2.7).

$$\begin{aligned} \tau_n &= (4.1 \pm 0.09)\mu\text{s} \\ D_n &= (113 \pm 11)\text{cm}^2/\text{s} \\ v = \mu_n E &= (537.1 \pm 0.7)\text{m/s} \end{aligned} \tag{2.7}$$

To calculate the moveability μ_n we have to use $E = U/l = (50.4 \pm 2)\text{V}/(30.00 \pm 0.05)\text{mm}$.

$$\mu_n = \frac{v}{E} = \frac{v \cdot l}{U} = (3200 \pm 130)\frac{\text{cm}^2}{Vs} \tag{2.8}$$

where the Gaussian error propagation

$$s_{\mu_n} = \mu_n \sqrt{\left(\frac{s_v}{v}\right)^2 + \left(\frac{s_l}{l}\right)^2 + \left(\frac{s_U}{U_{\text{ext}}}\right)^2}$$

was used.

Unfortunately this means only the diffusion constant D_n agrees within the standard deviation with the values from the literature[3] which are $\tau = (45 \pm 2)\mu s$, $D = 101\text{cm}^2/\text{s}$ and $\mu = 3900\text{cm}^2/\text{Vs}$. The discussion of possible systematic errors follows in 2.4.

2.3.2 Variation of External Electrical Field E

In this part we have measured the needle voltage $U_{E,x}(t)$ for a fixed distance $x = 3.2\text{mm}$ but for several different external electrical fields $E = U/l$. The problem is the same, that $U_{E,x}(t)$ is not a Gaussian. The solution is also the same, but here it is less intuitive and more abstract. For every point in time t we will have a function $U_{t,x}(E)$. Comparing this with the modeled physical process (2.1) we get

$$U_{t,x}(E) = Ae^{-\frac{t}{\tau_n}} \cdot \frac{1}{\sqrt{4\pi D_n t}} \exp\left(-\frac{(x-\mu_n E t)^2}{4D_n t}\right) \tag{2.9}$$

$$= Ae^{-\frac{t}{\tau_n}} \cdot \frac{1}{\sqrt{4\pi D_n t}} \exp\left(-\mu^2 t^2 \frac{(\frac{x}{\mu_n t} - E)^2}{4D_n t}\right) \tag{2.10}$$

$$= \frac{A}{\mu_n t} e^{-\frac{t}{\tau_n}} \cdot \frac{1}{\sqrt{2\pi \frac{2D_n t}{\mu^2 t^2}}} \exp\left(-\frac{(\frac{x}{\mu_n t} - E)^2}{2 \cdot \frac{2D_n t}{\mu_n^2 t^2}}\right) \tag{2.11}$$

So when we fit $U_{x,t}(E)$ with a Gaussian

$$U_{t,x}(E) = A(t) \frac{1}{\sqrt{2\pi\sigma^2(t)}} \exp\left(-\frac{(E - E_c(t))^2}{2\sigma^2(t)}\right) \tag{2.12}$$

the following relations arise

$$\begin{aligned} E_c(t) &= \frac{x}{\mu_n t} \\ \sigma^2(t) &= 2\frac{D_n}{\mu_n^2 t} \quad \text{where } \mu \text{ has to be taken from the } E_c\text{-fit} \\ A(t) &= \frac{A}{\mu_n t} e^{-\frac{t}{\tau}} \end{aligned} \tag{2.13}$$

An example of the Gaussian fits of the raw data $U_{E,x}(t)$ to calculate the offset of the shifted output is shown in 2.7. The transformed data $U_{x,t}(E)$ is shown in figure 2.8. The meaning of this plot is very unintuitive, but according to the model (2.1) this is a Gaussian. The error of the external field s_E is due to the uncertainties of the applied voltage $s_U = 2\text{V}$. The error of the length l of the semi conductor can be neglected. So the error of the external electrical field is $s_E = s_U/l$ which is shown in figure 2.8.

With the same method which we used in the previous section we get the diagrams for $A(t)$, $\sigma(t)$ and $E_c(t)$. These are shown in the figures 2.9, 2.10 and 2.11 where the appropriate fits from (2.13) were made. Again we had to use filter rules. We applied the rule $t \in [10\mu\text{s}, 1\text{s}] \wedge E \in [\frac{20}{30}\text{V/mm}, \frac{50}{30}\text{V/mm}] \wedge \sigma \in [0, 2\text{V/mm}] \wedge A \in$

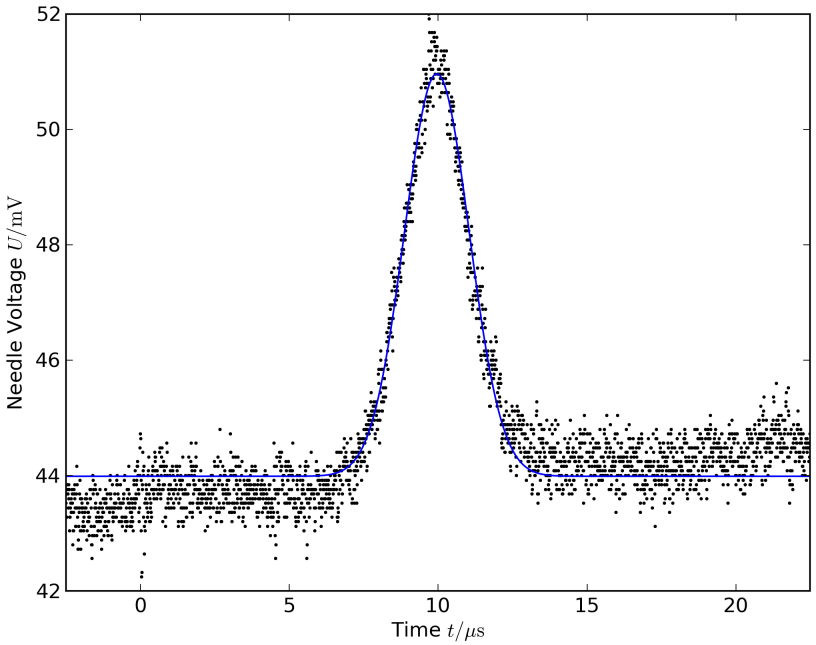

Figure 2.7: Example of our measured curves $U(t)$ for $E = 44\mathrm{V}/30\mathrm{mm} \approx 1.47\mathrm{V}/\mathrm{mm}$ with a Gaussian fit.

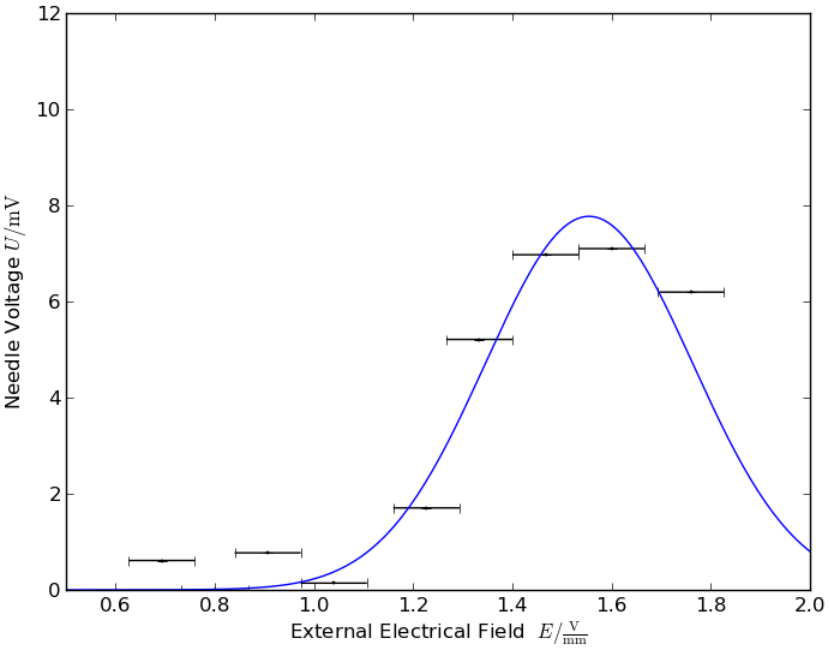

Figure 2.8: Example of the transformed function $U(E)$ for $t = 10.02\mu\mathrm{s}$.

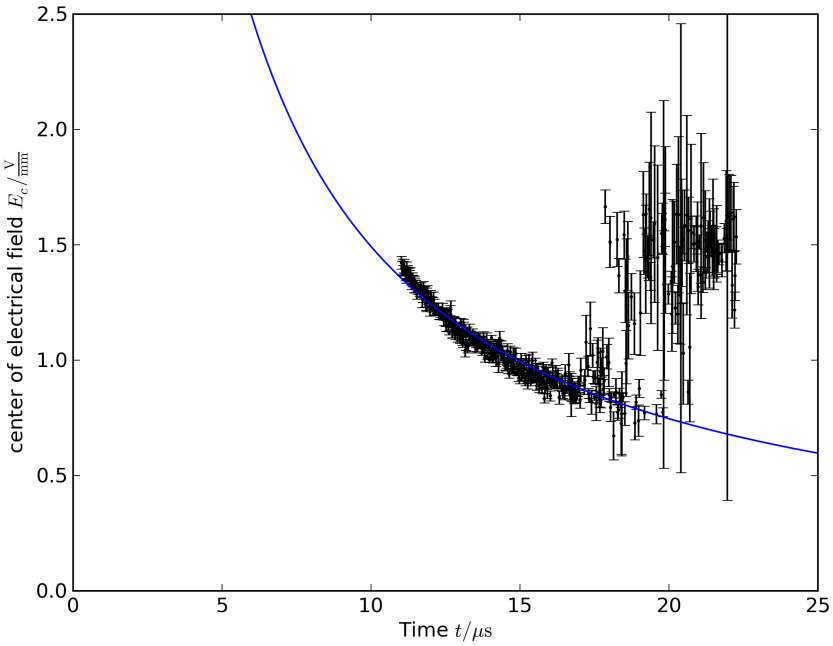

Figure 2.9: Center of electrical field with the appropriate fit.

$[0, 5\mathrm{V}^2/\mathrm{mm}]$. And again looking at the plots, one sees that the rules have not been to strict.

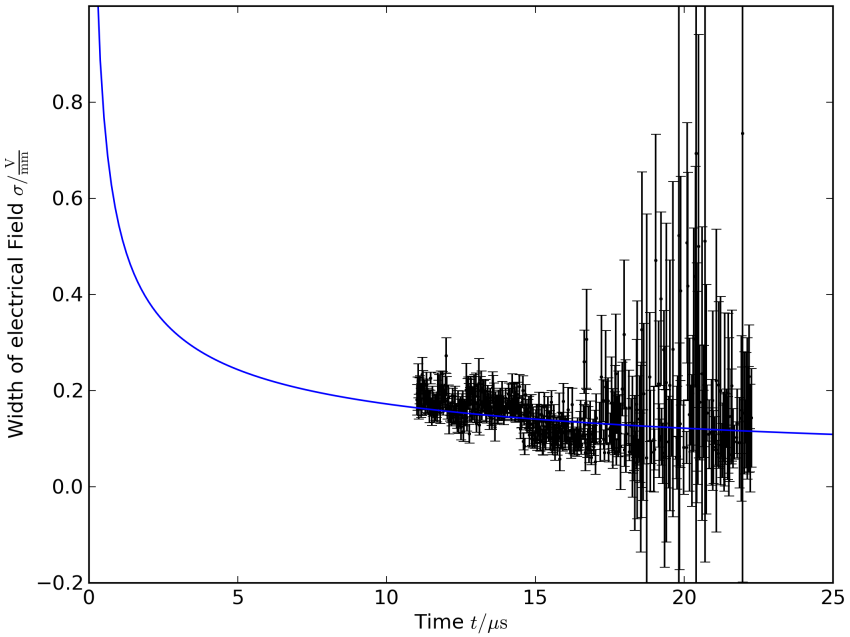

Figure 2.10: 'Widening' of the electrical field with the appropriate fit.

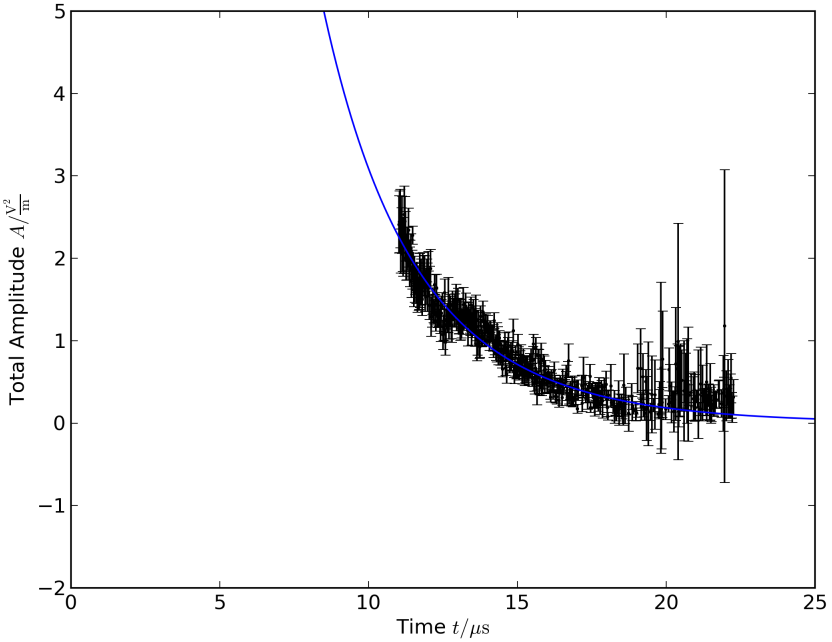

Figure 2.11: Time evolution of the recombination with the appropriate fit.

The fits have produces the following results.

$$\begin{aligned} \tau &= (4.71 \pm 0.1)\mu\text{s} \\ D_n &= (133 \pm 3)\text{cm}^2/\text{s} \\ \mu_n &= (2994 \pm 13)\text{cm}^2/\text{Vs} \end{aligned} \tag{2.14}$$

2.4 Discussion of the Results

The moveabilities μ_n that we have measured are too small compared to literature values. The lifetimes are much to small (by a factor of 10). The diffusion constant D_n is roughly in agreement with the literature value [3].[4] In the following section we will discuss a few sources of errors which could have afflicted our measurements.

The surface of the semi conductor could be defiled. This means the impurities could reflect or absorb light from the laser. When the laser is moved to different spots of the surface, the energy used to lift electrons into the conducting band varies. This will afflict our results. This will systematically lower or raise the points individually in the $U_{E,t}(x)$ plots, for example figure 2.3. Because of the transformation, it is difficult to foretell how this afflicts the values of our results.

On the other hand, impurities inside the semi conductor can change the physical/electrical properties such as movability, diffusion constant, and life time of electrons. Depending on the material and the concentration this could change our results in both direction.

A big problem with the transformation is, that the Gaussian fits are made to curves with only about 10 points, which scatter around the real values. As state already above, some fits were very bad, so we had to apply filtering rules. But even after that the 'good' fits aren't that trust worthy. This could change our values in both direction.

2.5 Conclusion

The results of the two measurements are shown in table 2.3. Most of our results do not agree with the literature value within the standard deviations. For reasons refer to section 2.4. The value of the life time τ_n is in agreement with the value that other groups in the FP-I. May be the literature value from [3] is not correct.

[4] We search a different source for these values, but unfortunately the website of the National Institute of Standards and Technology is closed due to the fiscal cliff in the USA and the paper 'The Mobility and Life of Injected Holes and Electrons in Germanium', Phys. Rev. 81, 835–843 (1951) by J. R. Haynes and W. Shockley is not available in the library.

	x variated	E variated	Literature[3]
Life time τ_n	$(4.1 \pm 0.09)\mu$s	$(4.71 \pm 0.1)\mu$s	$(45 \pm 2)\mu s$
Diffusion constant D_n	$(113 \pm 11)\text{cm}^2/\text{s}$	$(133 \pm 3)\text{cm}^2/\text{s}$	$101\text{cm}^2 s$
Moveability μ_n	$(3200 \pm 130)\frac{\text{cm}^2}{\text{Vs}}$	$(2994 \pm 13)\text{cm}^2/\text{Vs}$	$3900\text{cm}^2/\text{Vs}$

Table 2.3: Overview of our measurement results and the literature values.

Part 3

Semiconductor Detector

3.1 Introduction

3.1.1 Set-Up

We have two samples serving us as source of nuclear radiation. One is Cobalt (^{57}Co) the other is Americium (^{241}Am). The emitted radiation hits a detector made from a semiconducting material as shown in figure 3.1. Also we have two types of semicondutors: a silicon and a CdTe-semiconductor. Whichever we use the detector will give the signal to a preamplifier. This transmits it to a shaping amplifier. The so modified signal continues to Multi Chanal Analyser (MCA). It separates the events with different energies, assigns them to a so called channel. The counted events are given to a computer which stores the data into a file.

3.1.2 Theoretical Basics

Calibration Line

The Multi-Channal-Analyser sorts ranges of energy into channels. Now it is up to us to find out the relationship between channel and energy. We know that this

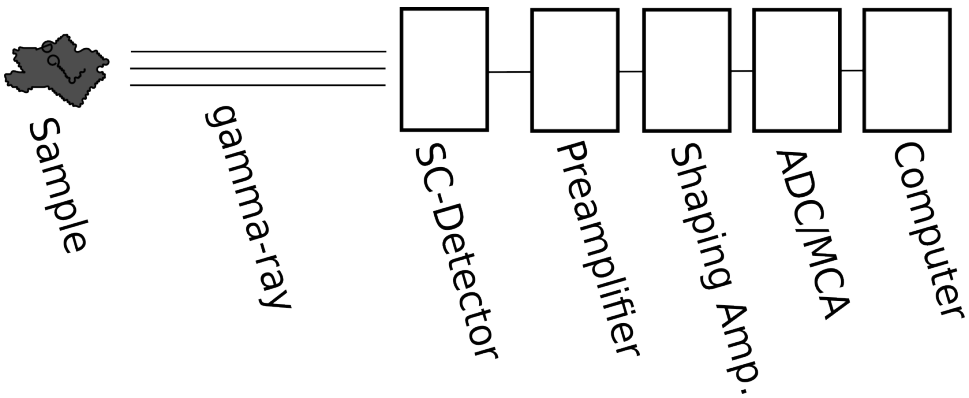

Figure 3.1: Set-Up of the third experiment: semiconductor detector.

relationship is linear. That leads to a linear equation.

$$E(C) = m \cdot C + b \tag{3.1}$$

Here C is the channel, E the energy and m and b two free parameters which we need to determine.

Proportion of Absorption

In the Manual [3] it is given for the proportion

$$P = \frac{Abs_{Si}}{Abs_{CdTe}} = \frac{A_{Si}/a_{Si}}{A_{CdTe}/a_{CdTe}} \tag{3.2}$$

Here A_{CdTe} stands for the absorbed photons and a_{CdTe} for the size of the conductor. Same applies for $A_{Si}$and a_{Si}. In the manual it is given

$$a_{Si} = 100\text{mm}^2$$
$$a_{CdTe} = 23\text{mm}^2$$

Relativ Energy Resolution

To get the resolution from a spectrum one need to use the formula given in the manual [3].

$$\text{RER}(E) = \frac{\text{FWHM}(E)}{E} \tag{3.3}$$

With E the energy and FWHM the full width at half maximum.

3.2 Measurement

First we measured the Cobalt sample because the other group of the short-half-time-experiment needed it.

Detector	Time	Sample	File
Si	1h	^{57}Co	`Si_ Co.mca`
$CdTe$	1h	^{57}Co	`CdTe_ Co.mca`
Si	1h	^{241}Am	`Si_ Am.mca`
$CdTe$	1h	^{241}Am	`CdTe_ Am.mca`
Si	1h	empty	`Si_ Unter.mca`
$CdTe$	1h	empty	`CdTe_ Unter.mca`

3.3 Evaluation

First we had to subtract the underground from our data. In all our calculations we need not to calculate the count rates (counts per time) because the measurement

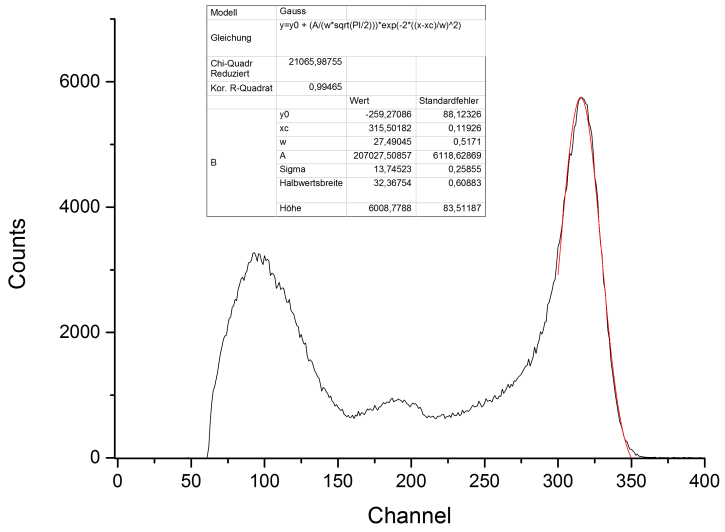

Figure 3.2: Gauss-fit of the spectrum of the Americium sample taken with the CdTe-semiconductor

duration was the same for all measurements.

3.3.1 Calibration of Channels

CdTe-Semiconductor

We used Origin to fit the lines of the measured spectra. See figure 3.2 and 3.3. For the CdTe-semiconductor we found the values shown in table 3.1. With this

	Channel	Energy/keV [3]
Co_1	(621 ± 14)	122.06
Co_2	(694 ± 8)	136.47
Am	(315 ± 13)	59.5

Table 3.1: Result of the fits for the Calibration-Line of the CdTe-Conductor

data and (3.1) we come to the calibration line which assigns each channel an energy range as shown in figure 3.4.

$$E(C) = (0.2030 \pm 0.0019)\text{keV} \cdot C - (4.4 \pm 1.1)\text{keV} \tag{3.4}$$

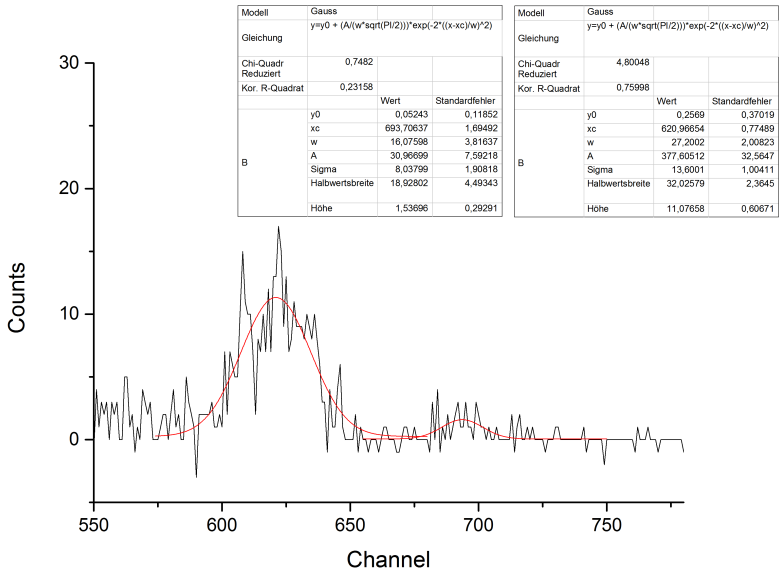

Figure 3.3: Gauss-Fit of the spectrum of the Cobalt sample taken with the CdTe-semiconductor

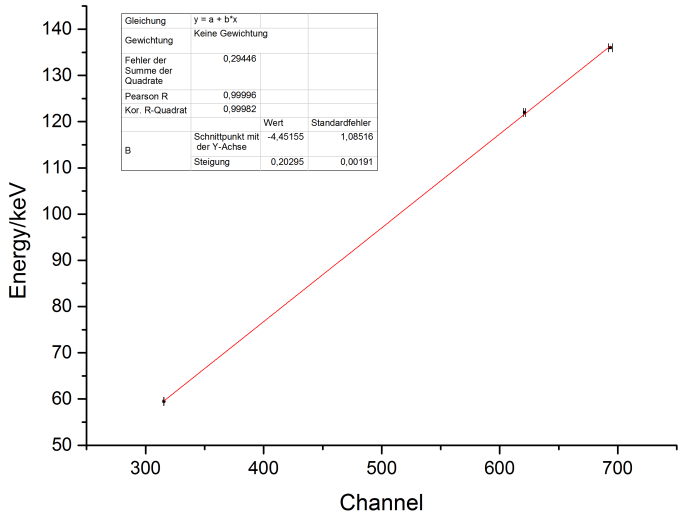

Figure 3.4: Linear fit of the data from table 3.1 for the calibration

Si-Semiconductor

The same way we got the calibration of the Si-Conductor. The plots and tables are in the attachment.

$$E(C) = (0.196 \pm 0.0003)\text{keV} \cdot C + (0.18 \pm 0.18)\text{keV} \tag{3.5}$$

3.3.2 Proportion of Absorption

With (3.2) and the data from the fits we can find out the proportion of absorption We receive the error with Gaussian error propagation through

	Counts of $CdTe$-Conductor	Counts of Si-Conductor	P (3.2)
Co_1	(380 ± 30)	(370 ± 30)	$(0,2239 \pm 0,03)$
Co_2	(31 ± 8)	(26 ± 7)	$(0,2671 \pm 0,09)$
Am	(207000 ± 611)	(16900 ± 300)	$(0,0188 \pm 0,0003)$

Table 3.2: Collected data from fits and result of proportion

$$\sigma_P = \sqrt{\left(\frac{a_{CdTe}}{a_{Si} \cdot A_{CdTe}} \cdot \sigma_{Si}\right)^2 + \left(\frac{A_{Si} \cdot a_{CdTe}}{a_{Si} \cdot A_{CdTe}^2} \cdot \sigma_{CdTe}\right)^2} \tag{3.6}$$

3.3.3 Relative Energy Resolution

From the fits we get the FWHM of each Gaussian. But first we need to transform them from channel- to energy. We can do that with the calibrations from 3.3.1. Herefrom we get following data with the result in the last column.

CdTe-Detector	FWHM(C)	FWHM(E)/keV	E/keV	RER(E) from (3.3)
Co_1	(32 ± 2)	(6.5 ± 0.4)	122.06	(0.053 ± 0.003)
Co_2	(19 ± 4)	(3.9 ± 0.8)	136.47	(0.028 ± 0.006)
Am	(32.4 ± 0.6)	(6.58 ± 0.14)	59.5	(0.111 ± 0.002)

Table 3.3: Collected data for calculation of Relative Energy Resolution(RER) of the CdTe-semiconductor

For this calculations we used the Gaussian errors propagation

$$\sigma_{\text{FWHM}(E)} = \sqrt{(m \cdot \sigma_{\text{FWHM}(C)})^2 + (\text{FWHM}(C) \cdot \sigma_m)^2} \tag{3.7}$$

$$\sigma_{\text{RER}} = \frac{1}{E} \cdot \sigma_{\text{FWHM}(E)} \tag{3.8}$$

On the very same way we came to the results of the Si-conductor.

Si-Detector	RER(E) from (3.3)
Co_1	(0.050 ± 0.003)
Co_2	(0.024 ± 0.006)
Am	(0.0906 ± 0.0017)

Table 3.4: Relative Energy Resolution(RER) of the Si-semiconductor

3.4 Conclusion

3.4.1 Calibration Line

We found the peaks and could get the calibration lines from it. They are as follows.

$$E_{CdTe}(C) = (0.2030 \pm 0.0019)\text{keV} \cdot C - (4.4 \pm 1.1)\text{keV} \tag{3.9}$$

$$E_{Si}(C) = (0.196 \pm 0.0003)\text{keV} \cdot C + (0.18 \pm 0.18)\text{keV} \tag{3.10}$$

If one takes a look on the figure 3.4 he can see that we are within the errors. Even with very poor data (=peaks not clearly distinguishable from underground) the result is surprisingly good. In 3.10 we even hit the origin.

3.4.2 Proportion

Our results for the proportion between the absorption of the CdTe- and the Si-semiconductor are shown in the table 3.5 next to the given values [3]. Here for the first time the poor data mentioned before draws attention. The proportion of the two Co-peaks is far out of the errors. For the Americium things seem better but still not within the standard deviations. We did not expect to get better results because

Peak	measured	given [3]
Co_1	$(0,2239 \pm 0,03)$	0,0183
Co_2	$(0,2671 \pm 0,09)$	0,022
Am	$(0,0188 \pm 0,0003)$	0,0140

Table 3.5: comparison of measured and given values of the proportion

of this data. If someone measures a peak with 31 counts he can not expect to get better results. For better results we would need to do much longer measurements. Unfortunately this is not possible because we had only spare time at the setting.

3.4.3 Relative Energy Resolution

Our results of the relative energy resolution are visible in table 3.6. Especially here

RER(E)	CdTe-Detector	Si-Detector
Co_1	$(0,053 \pm 0,003)$	$(0,050 \pm 0,003)$
Co_2	$(0,028 \pm 0,006)$	$(0,024 \pm 0,006)$
Am	$(0,111 \pm 0,002)$	$(0,0906 \pm 0,0017)$

Table 3.6: Relative Energy Resolution(RER) of the Si- and CdTe-Semiconductor

again we witness the consequence of the small amount of data in the Co-Peaks. Still one can see that the RER of the CdTe-Detector is higher, as we expected.

Appendix A

Part I

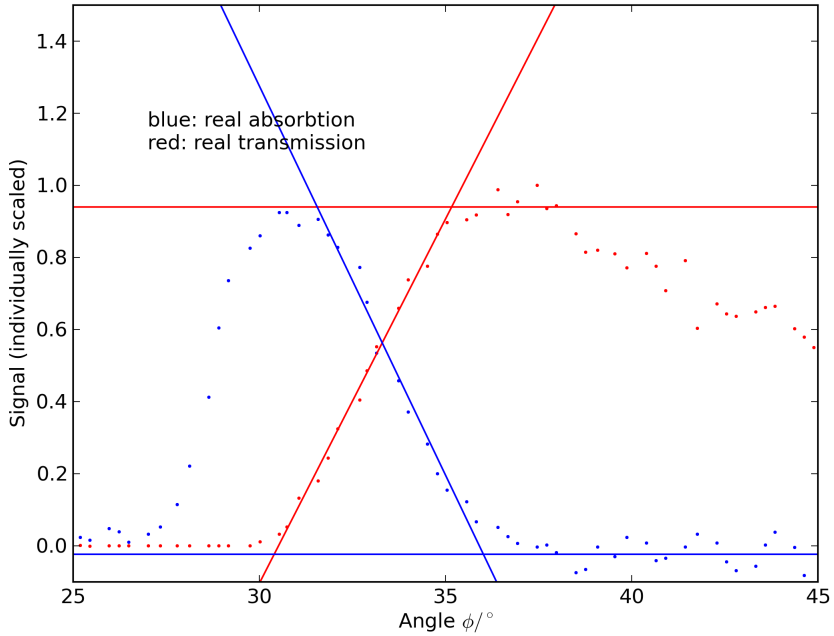

Figure A.1: Absorption and transmission spectra normalized and zoomed to the right intersection of the CdTe-semiconductor

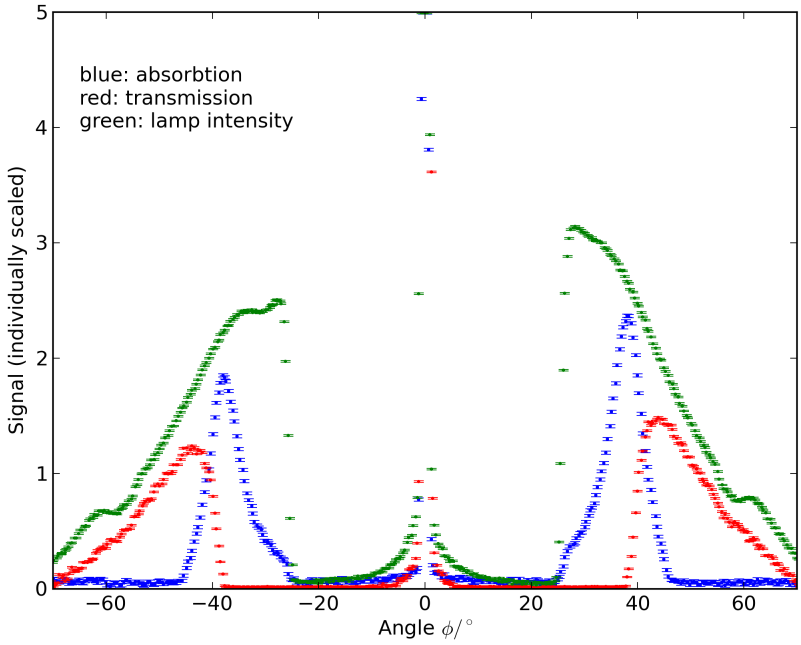

Figure A.2: Plot of all data as we received it from the computer for the Si-semiconductor

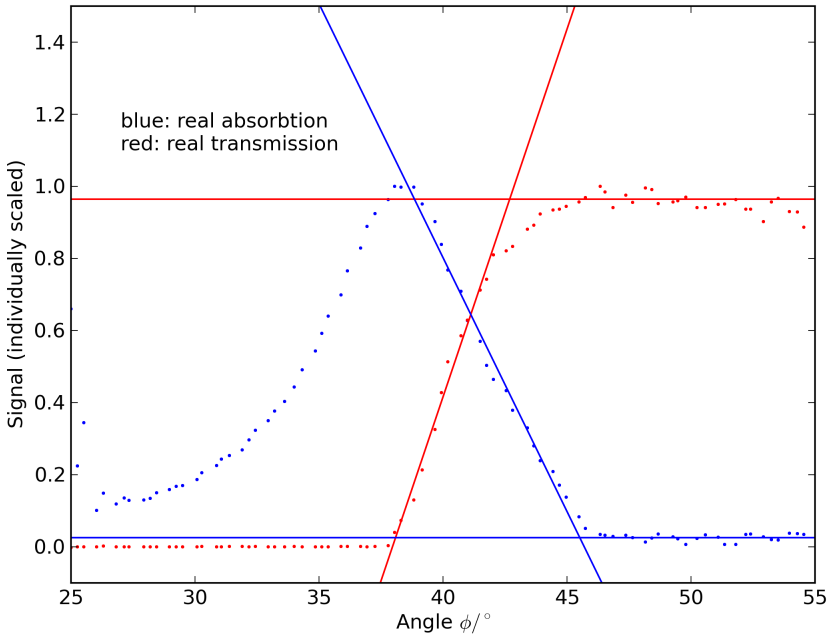

Figure A.3: Absorption and transmission spectra zoomed to the right intersection of of the Si-semiconductor

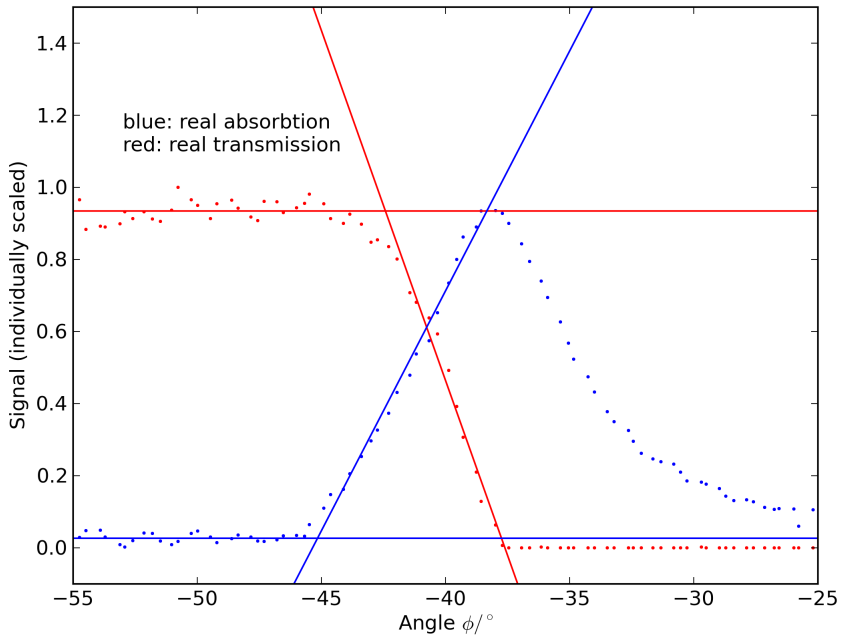

Figure A.4: Absorption and transmission spectra normalized and zoomed to the left intersection of the Si-semiconductor

Appendix C

Part III - Si

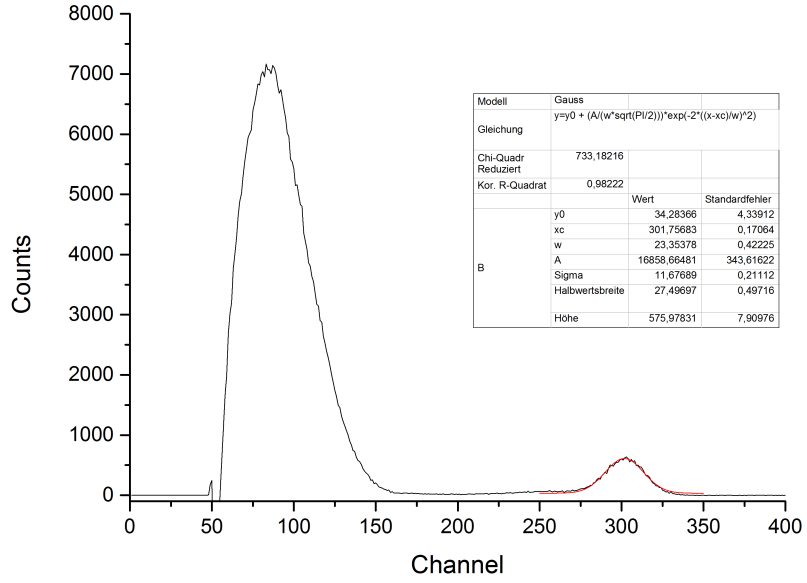

Figure C.1: Gauss-fit of the spectrum of the Americium sample taken with the Si-semiconductor

	Channel	Energy/keV [3]
Co_1	(620 ± 13)	122,06
Co_2	(694 ± 7)	136,47
Am	(302 ± 12)	59,5

Table C.1: Result of the fits for the calibration line of the Si-semiconductor

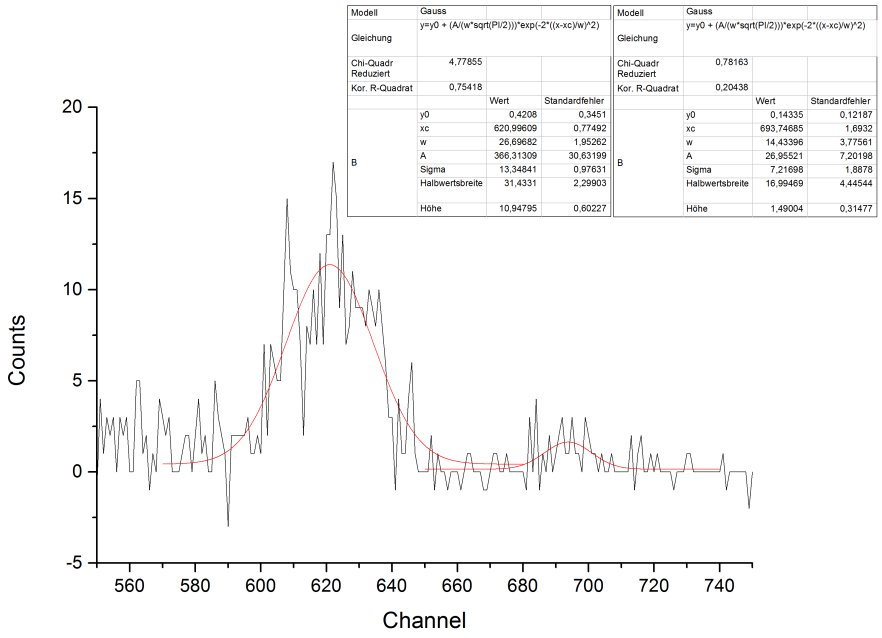

Figure C.2: Gauss-fit of the spectrum of the Cobalt sample taken with the Si-semiconductor

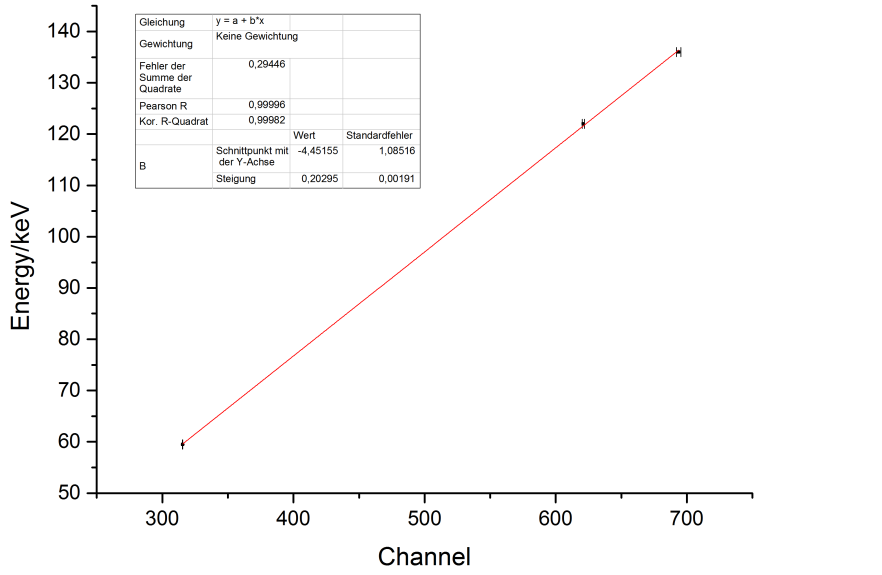

Figure C.3: Linear fit of the data from table C.1 for the calibration

Bibliography

[1] Simon Amrein. Halbleiter & halbleiterdetektoren. Staatsexamensarbeit, Albert-Ludwigs-Universität Freiburg Physikalisches Institut, April 2008.

[2] Wolfgang Demtröder. *Experimentalphysik 3*. Springer, 4 edition, 2010.

[3] S.Amrein, K. Lohwasser, M. Köhli, and S. Kühn. Versuchsanleitung fp i: Halbleiter, März 2013.